Annals of Glaciology 58(75pt1) 2017 doi: 10.1017/aog.2017.24

Structural provinces of the Ross Ice Shelf, Antarctica

Christine M. LEDOUX,[1] Christina L. HULBE,[2] Martin P. FORBES,[2] Ted A. SCAMBOS,[3] Karen ALLEY[3]

[1]*Department of Geology, Portland State University, Portland, OR 97215, USA*
[2]*School of Surveying, University of Otago, Dunedin, New Zealand.*
E-mail: christina.hulbe@otago.ac.nz
[3]*National Snow and Ice Data Center, University of Colorado Boulder, Boulder, CO, USA*

ABSTRACT. The surface of the Ross Ice Shelf (RIS) is textured by flow stripes, crevasses and other features related to ice flow and deformation. Here, moderate resolution optical satellite images are used to map and classify regions of the RIS characterized by different surface textures. Because the textures arise from ice deformation, the map is used to identify structural provinces with common deformation history. We classify four province types: regions associated with large outlet glaciers, shear zones, extension downstream of obstacles and suture zones between provinces with different upstream sources. Adjacent provinces with contrasting histories are in some locations deforming at different rates, suggesting that our province map is also an ice fabric map. Structural provinces have more complicated shapes in the part of the ice shelf fed by West Antarctic ice streams than in the part fed by outlet glaciers from the Transantarctic Mountains. The map may be used to infer past variations in stress conditions and flow events that cannot be inferred from flow traces alone.

Keywords: crevasses, ice shelves, structural glaciology

INTRODUCTION

Linear features observed at the surface of a flowing ice mass represent an integrated history along the flow trajectory. In an ice shelf, that history includes variation in flow of tributary glaciers, conditions at the coastline where the ice went afloat, and processes within the floating ice (see Fahnestock and others, 2000; Glasser and others, 2009, 2015; Ely and Clark, 2016). Linear features include both along-flow-oriented flow stripes and crevasses whose presence and geometry are determined by principal stresses in the ice (e.g. McGrath and others, 2012; Colgan and others, 2016). Flow stripes at the surface can be traced back upstream to source regions and, together with textures due to crevasses, can be used to identify regions with common history and to infer deformation history of the ice within each region.

Surface features record ice shelf history in different ways. Once formed, flow stripes and crevasses are transported toward the calving front. Because the flow field is neither spatially nor temporally uniform, the features experience spatially and temporally varying stress and strain conditions. This gives rise to time-varying deformation that may be interpreted in terms of past variability. For example, streaklines are surface undulations associated with flow variations in grounded source ice (Glasser and others, 2015). Once afloat, these flow features become passive tracers and their deformation relative to the modern flow field has in the case of the Ross Ice Shelf (RIS), been used to infer past flow variability (Jezek, 1984; Casassa and others, 1991; Fahnestock and others, 2000; Hulbe and Fahnestock, 2007).

In the present contribution, we consider flow stripes and crevasse patterns together, in order to consider deformation in the ice shelf more completely. Glacier ice undergoes brittle fracture at sufficiently large stresses (cf. Rist and others, 1999). Fractures nucleate in the subsurface (Nath and Vaughan, 2003) and when stress intensity at a crack tip is large enough, the crack will propagate in response to both the ambient stress field and near-field modifications to that field arising from the fractures themselves. Material properties of the ice may modify its fracture toughness and thus either promote or suppress propagation (Khazendar and others, 2007; Glasser and others, 2009; Hulbe and others, 2010; Borstad and others, 2012). Most crevasses visible at the surface remain relatively short over most of the advective pathway, and only become long (and thus the failure planes for large icebergs) in the near-front environment, an effect that can be related to both material properties and the interaction among nearby fractures (cf. Lazzara and others, 1999; Hulbe and others, 2010; Brunt and others, 2011).

Our primary interest is in the horizontal expression of fracture propagation as a mixed-mode opening (mode I) and sliding (mode II) phenomenon and governed by conditions within the ice shelf. Once initiated, crevasses are advected in the flow field and may change orientation or shape depending on the stress field encountered along the way. As passive features, crevasses may be rotated, elongated, closed or otherwise modified by the viscous flow of the ice. They may also be buried by new snow. Where crevasses continue to propagate or are reactivated during advection, their shapes record stresses experienced along the path and perhaps also changes in the ice shelf (MacAyeal and Lange, 1988; Hulbe and Fahnestock, 2007).

The analysis presented here begins with a feature map of the RIS created using moderate resolution images of the ice shelf surface. Crevasse geometries are classified in a scheme that emphasizes what they reveal about principal stress orientations. Next, structural provinces (Jackson and Kamb, 1997; Herzfeld and others, 2013) within the ice shelf are classified according to pervasive crevasse patterns within regions. Comparison with remotely sensed, present-day strain rates, principal stresses, and ice thickness allow us to discuss ways in which structural provinces may be used to learn about both past and present conditions on the ice shelf.

https://doi.org/10.1017/aog.2017.24 Published online by Cambridge University Press

DATA

Image mosaics

Clear feature geometries that are straightforward to digitize are required for mapping crevasse patterns and regional surface textures. We are interested in groups of features with similar orientations, which produce textures at the ice surface that persist over tens of km rather than finer, sub-km scale, details. While automated approaches exist (Ely and Clark, 2016), we hand-digitize features with the intention of developing familiarity with the textures and the mechanical settings in which they are produced. These objectives make moderate resolution optical images suitable for our work.

Two image mosaics are the primary data sources for our map: the first epoch of the MODIS (Moderate Resolution Imaging Spectroradiometer) Mosaic of Antarctica (MOA; Haran and others, 2005) and the Landsat Image Mosaic of Antarctica (LIMA; Bindschadler and others, 2008). The first epoch of the MOA is a composite of 260 individual MODIS images acquired between 20 November 2003 and 29 February 2004 with an effective resolution of 125 m. The LIMA, which has a resolution of 30 m and covers the ice shelf region north of about 82° S, is a composite of nearly 1100 images acquired by the Landsat ETM+ (Enhanced Thematic Mapper Plus) sensor between 1999 and 2003. Because the MOA composite amplifies shadows, low-relief features like along-flow lineations, sagging snow bridges, and regional textures arising from snow-covered features are readily apparent in the mosaic. We thus use the MOA to make an initial mapping of the whole ice shelf surface and turn to the higher resolution LIMA and some individual Landsat 8 scenes, obtained via the USGS EarthExplorer (earthexplorer.usgs.gov), to resolve ambiguities regarding boundaries of some textured regions.

Velocity, strain rates and stresses

Glaciological strain rates and stresses, computed using remotely sensed surface velocity, are used to support interpretation of the feature maps. We compared two velocity products, the InSAR-derived MEaSUREs data set (Rignot and others, 2011) and a Landsat-8-derived velocity computed by correlating grey scale patterns in small sub-scenes between sequential images collected between 1 October 2014 and 31 March 2015 (Fahnestock and others, 2016). The former covers the entire RIS, while the latter has a southern limit of 82.65° S.

Strain rates are approximated as horizontal gradients of the two dimensional velocity field. We compute effective strain rates $\dot{\epsilon}_e$ as the second invariant of the strain rate tensor

$$\dot{\epsilon}_e^2 = \frac{1}{2}\dot{\epsilon}_{ij}\dot{\epsilon}_{ij} \quad (1)$$

in which the subscripts i,j represent three orthogonal directions. Vertical shearing (the vertical gradient of horizontal velocity components) is negligible in the floating ice shelf and the vertical normal strain rate is calculated from the horizontal divergence ($\dot{\epsilon}_{zz} = -\dot{\epsilon}_{xx} - \dot{\epsilon}_{yy}$).

Artifacts and errors in both data sets are amplified by the gradient calculation. These appear as linear features associated with image edges, circuitous shapes associated with clouds and as noise. Comparing the two effective strain rate results, we prefer the Landsat-8-derived field for its sharper and more easily managed artifacts. Uncertainty in the Landsat-8-derived velocity field is 5 m a^{-1} and the propagated uncertainty on the effective strain rate, using gradients computed on a 750 m regular grid, is 0.008 a^{-1}. This is similar to errors reported for MEaSUREs. The estimated error does not capture noise in the effective strain rate field. The $1-\sigma$ standard deviation in the $\dot{\epsilon}_e$ field downstream of the large outlet glaciers discussed in a later section is 0.016 a^{-1}.

Deviatoric stresses are computed as $\sigma'_{ij} = \sigma_{ij} - (1/3)\sigma_{ij}\delta_{ij}$ in which δ_{ij} is the Kronecker δ. The stress tensor σ_{ij} is estimated using the finite strain rates ϵ_{ij} and the inverse form of the generalized flow law for ice

$$\sigma_{ij} = B\dot{\epsilon}_e^{(1/n)-1}\dot{\epsilon}_{ij} \quad (2)$$

in which the exponent n is equal to 3. We use a value of 760 kPa $a^{-1/3}$ for the temperature-dependent rate factor B, equivalent to a depth average temperature of 247 K (Van der Veen, 1999, p. 16). Principal stress directions and magnitudes are computed as the eigenvectors and eigenvalues of deviatoric stress tensor. The uniform rate factor is very simple, but our interest is in the eigenvector directions rather than the values.

Ice surface elevation

We use the Digital Elevation Model-derived from measurements made by the Geoscience Laser Altimeter (GLAS) (DiMarzio, 2007) to supplement the discussion of ice shelf provinces. In general, thicker ice floats higher in the ocean surface but we do not convert the surface elevation into thickness because we lack knowledge of spatial variation in snow density and because this is not necessary for the intended use of the data.

METHODS

A wealth of surface features are visible in the MOA and LIMA mosaics, including streaklines, crevasses and through-cutting rifts. We began by digitizing prominent streaklines and crevasses as individual linear traces observed in the MOA (Fig. 1). Crevasses appear in the images either as sharp, sunlit/shadowed faces or as shadows cast within sagging snow bridges (Merry and Whillans, 1993). This means that our approach is blind to features that have yet to open across the fracture plane.

The crevasse map is not exhaustive. We digitized major features and groups of features that facilitate our ambition to create a structure map of the ice shelf. The first draft of the map was checked by comparison with the LIMA and individual Landsat 8 scenes. Crevasses with similar geometries were then grouped by type, and a relative sense of time was incorporated into the scheme by distinguishing between *initial crevasse geometries* that represent the early part of a fracture's history and thus are simple to interpret and *advected crevasse geometries* that arise from additional propagation along the advective path.

Initial geometries

1. *Transverse* geometries form where grounded ice goes afloat and longitudinal stress gradients are large. The

https://doi.org/10.1017/aog.2017.24 Published online by Cambridge University Press

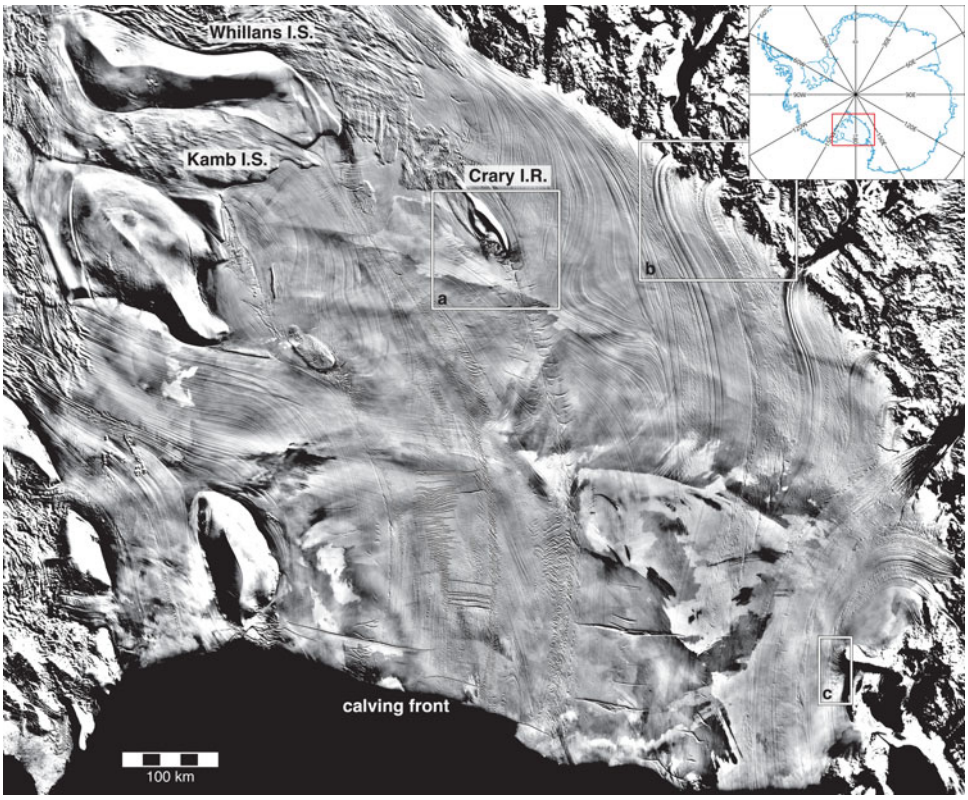

Fig. 1. The Ross Ice Shelf as it appears in the 2005 MODIS Mosaic of Antarctica (MOA). Areas described in more detail are (a) Crary Ice Rise, (b) coast of the Transantarctic Mountains between Beardmore and Nimrod Glaciers, (c) Minna Bluff.

initial geometry may be preserved during advection in a relatively uniform velocity field or rotated and elongated by gradients in the velocity field, even in the absence of additional propagation.

2. *Margin-Shear* geometries form in grounded ice due to simple shear in a relatively narrow zone near a sidewall (Fig. 2). Details in the shapes of margin-shear crevasses differ between glaciers and ice streams (see Merry and Whillans, 1993; Colgan and others, 2016), but the interest here is the broad scale surface texture rather than details. The overall orientation is upstream pointing, at an angle to the margin.

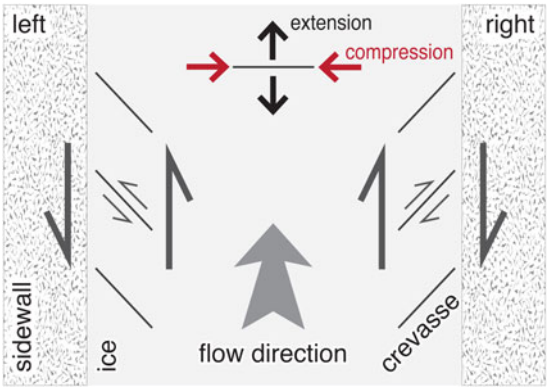

Fig. 2. Crevasses propagate in the most compressive principal stress direction. Shear stresses along the margins of glaciers and coastlines produce left and right margin-shear zones in which the sense of shear is as would be the case in other geologic settings. The resulting crevasses are upstream pointing, in the direction of maximum compression.

3. *Obstacle-Shear* geometries form where floating ice moves past features such as ice rises, coastal headlands and outlet corners of fjords. Stresses may be very large in these situations, resulting in vertical propagation through the full thickness of the ice and opening to form large rifts. The surface expression of these crevasses and rifts persist for long distances downstream (100s of kms), and the geometries often deform, rotating and elongating as they advect toward the shelf front.

Propagation during advection

Crevasses may maintain their initial geometry as they advect, either continuing to propagate or becoming passive features. They may also experience new episodes of propagation where the principal stress directions change, either due to advection or to near-field effects that arise as crevasse length grows. In such situations, the stress intensity is large enough to promote propagation but the initial geometry is poorly aligned with the local principal stress directions, so a new geometry emerges.

1. *Shear to Transverse* geometries develop when crevasses associated with shear past a lateral margin advect into a stress field favoring propagation transverse to flow (LeDoux, 2007; Hulbe and others, 2010). Long transverse rifts in the RIS originate as either *margin-shear* or *obstacle-shear* crevasses that subsequently propagate transverse to the ice flow direction in response to compression in the across-flow direction.
2. *Secondary* crevasses may develop at both high and low angles to the planes of larger crevasses in regions characterized by large shear strain rates. The crevasses form in response to relatively large shear stresses around the

https://doi.org/10.1017/aog.2017.24 Published online by Cambridge University Press

ends of the primary crevasses and are not cross-cutting. Both mode I and mode II fractures may form in situations like this (Martel and Boger, 1998; Kim and Sanderson, 2006).
3. *Tip Interaction* generates distinctive geometries indicative of near-field modification of the stress field (Cotterell and Rice, 1980; Pollard and Aydin, 1988). Crevasse tips may propagate in either a converging or diverging sense depending on the magnitude and orientation of the principal stresses and on the locations and geometries of other nearby fractures.
4. *Widening* geometries arise when stress conditions favorable to propagation exist but growth in the propagation direction is inhibited. This may occur at structural boundaries where ice properties affect the fracture toughness of the ice (Hulbe and others, 2010). In such circumstances, crevasses widen across the fracture plane.

Provinces

Structural provinces are adjacent regions with significantly different geologic structures (Jackson, 1997, p. 631). Following this, we define ice shelf structural provinces to be regions characterized by distinctive surface texture indicative of a common deformation history. That history, in turn, implies that ice material properties may vary across province boundaries. Because flow bands emerging from glaciers and ice streams are subject to new stress fields as they advect through the shelf, structural provinces should not necessarily replicate flow band boundaries. Here, ice shelf structural provinces are identified as regions with characteristic crevasse patterns and surface textures. Surface textures are most clearly expressed in the MOA because image stacking amplifies shadows cast by subtle features. Province boundaries were checked by comparison with the LIMA and Landsat 8. Examples are presented in the next section.

1. *Transverse Crevasse* provinces are characterized by linear features oriented approximately across flow. They contain ice that experienced significant longitudinal stretching (transverse compression) and vertical shortening downstream of a grounding line. This type of texture is most clearly identified and persistent in the eastern region of the RIS, where the shelf is fed by ice streams from the West Antarctic Ice Sheet.
2. *High Discharge* provinces are characterized by rough surface texture downstream of large outlet glaciers. This roughness is due to cross-cutting crevasses and across-flow undulations developed when the ice was grounded. Longitudinal flow stripes developed in the grounded ice may splay out or be rotated as the glacier flows into the ice shelf.
3. *Left and Right Margin-Shear* provinces are characterized by well-organized, initially upstream-pointing surface features that persist for long distances downstream. Margin-shear provinces arising from outlet glaciers may retain their original character, be rotated or overprinted as a glacier discharges into the ice shelf. New shear zone provinces may develop where floating ice flows around a headland or parallel to a coastline. We use the terms *left* and *right* to indicate the sense of shear, in the horizontal plane, where the texture originated.
4. *Suture Zone* provinces are characterized by surface textures that lack a clear preferred orientation. The simplest sutures form downstream of obstacles like ice rises. More complicated, composite suture zones form where several small outlet glaciers merge and turn together into the ice shelf.

PROVINCE MAP OF THE RIS

Our province map builds upon past analyses of the RIS (Fahnestock and others, 2000; Hulbe and Fahnestock, 2007) by synthesizing longitudinal flow features together with regional crevasse patterns and the structural provinces implied by them. For ease of examination, we present the map in two layers (Figs 3 and 4).

As defined here, the structural provinces are flowbands, or segments of flowbands, with a distinct surface texture from which the deformation history of the underlying ice can be inferred. Interpretation of surface texture is more straightforward in some regions than in others. Some textures and associated provinces persist over long distances, while elsewhere, initial textures are quickly lost and in some cases replaced by a new texture. The boundaries on the map are approximate and we have chosen to make a classification only where the evidence is clear.

Many Transantarctic Mountains (TAM) outlet glaciers experience an abrupt change in flow direction as they enter the ice shelf. As a result, crevasse patterns due to shear around outlet corners can be short lived, as ice turning past a corner enters into a region with different principal stresses. Where many small outlet glaciers merge, we classify one broad suture zone characterized by a mottled surface and no clearly preferred orientation of surface features.

Structural provinces are more readily identified in the western part of the RIS than in the east. This is due to the relatively more complex grounding zone in the east and the long history of ice stream discharge variability and ice rise formation in that region (see Hulbe and Fahnestock, 2007). We do not use streaklines to connect similar provinces along the flow direction because gaps may (or may not) represent past changes in ice shelf flow or spatial variation in the ambient stress field.

Crary Ice Rise

The region around Crary Ice Rise (CIR) is complicated by its geometry and by a history of ice flow variability (Fig. 5). Upstream-pointing crevasses due to shear form narrow bands along its shorelines. Other, more prominent, textures characterize the surrounding area. Outboard of the ice rise's northern shore, a broad region characterized by transverse crevasses is associated with discharge across the grounding line of the Whillans Ice Stream (WIS) ice plain. Between these we identify a province containing ice that was once in an ice stream shear zone. Downstream, older crevasses appear to be reactivated with complicated propagation directions that imply near-field modification of the stress field due to interactions among adjacent fractures. Textures are less clear to the south of the ice rise, until the ice shears by its downstream end, generating a distinctive set of what we have called an obstacle-shear initial geometry. These crevasses persist for a long distance downstream, carried along by the ice flow.

https://doi.org/10.1017/aog.2017.24 Published online by Cambridge University Press

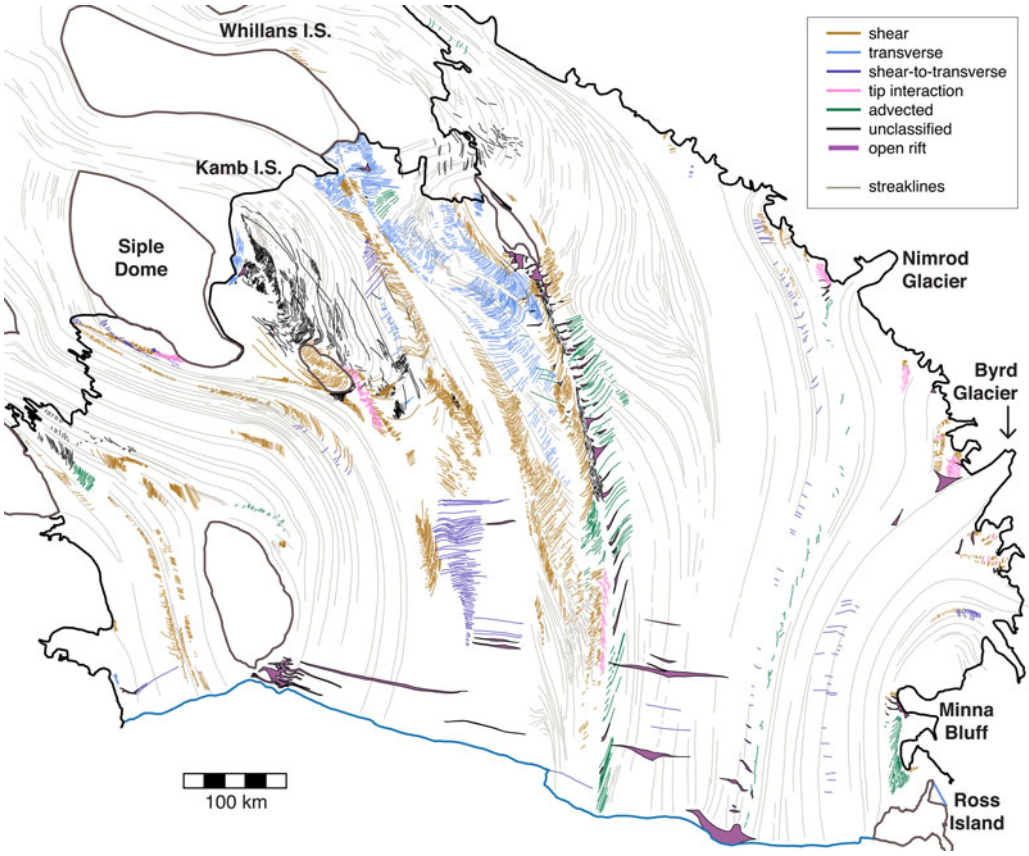

Fig. 3. Streaklines and crevasses digitized from the MOA, grouped and color coded by geometry.

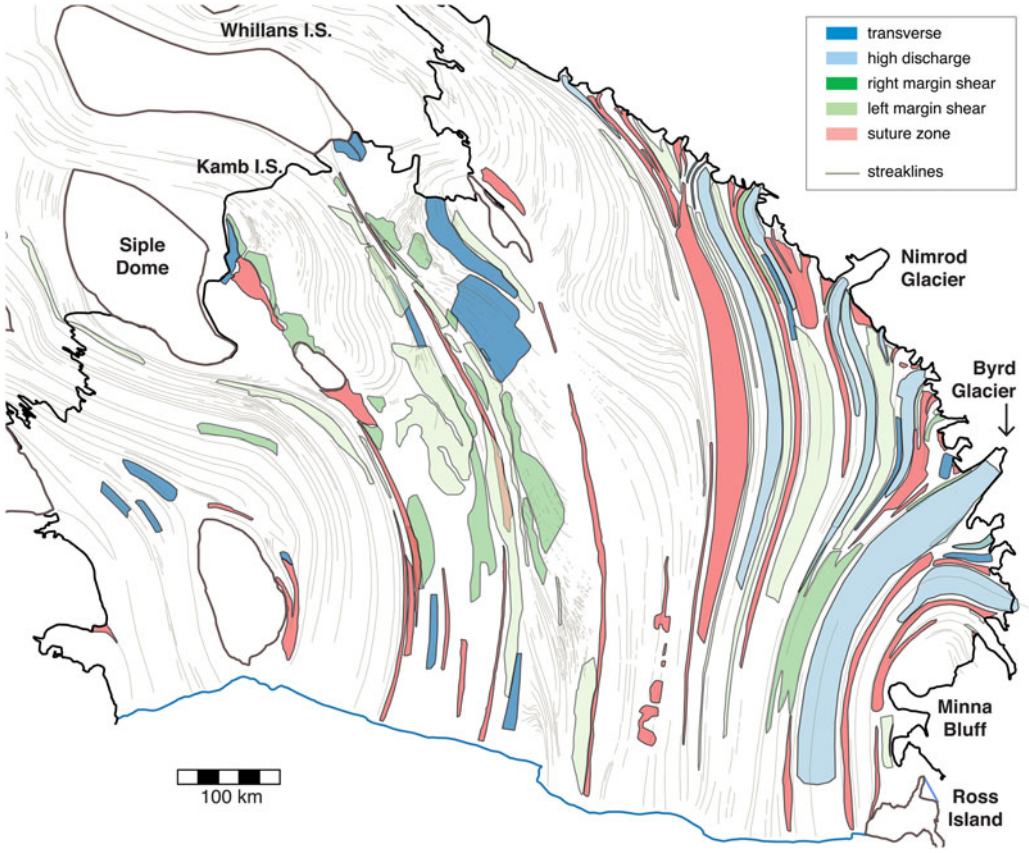

Fig. 4. Structural provinces identified according to surface texture in various flow bands within the RIS.

https://doi.org/10.1017/aog.2017.24 Published online by Cambridge University Press

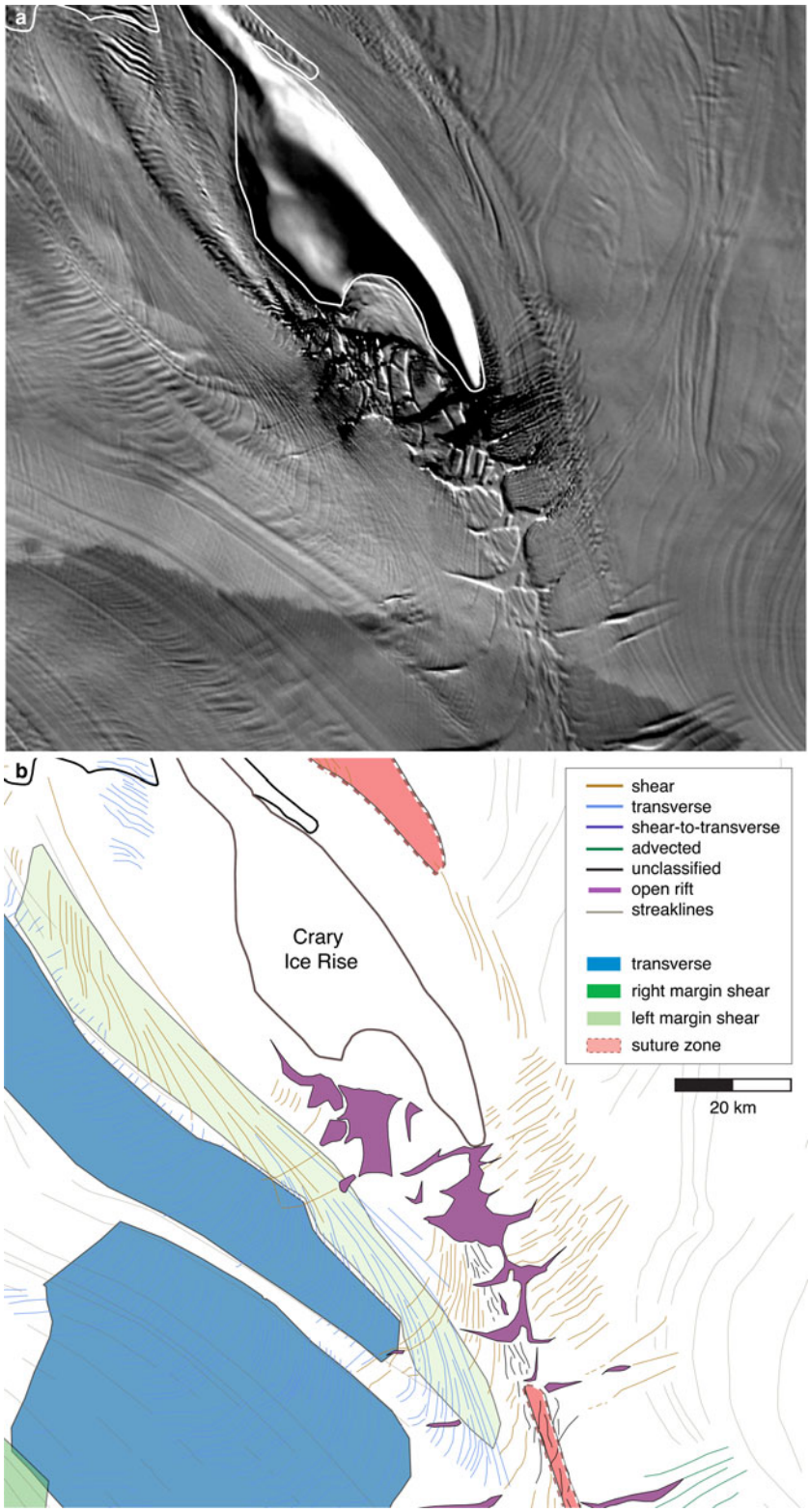

Fig. 5. The area around Crary Ice Rise, at the dowstream end of the Whillans Ice Stream ice plain. (a) Features as observed in the MOA. (b) Digitized streaklines and crevasses, with interpreted structural provinces.

Large open rifts form near the downstream end of CIR and a narrow suture zone forms between these. Crevasses and rifts along the flanks of the suture change shape as they advect toward the shelf front and in some locations new, smaller fractures are observed between the older, larger features. These crevasses are neither uniformly distributed nor uniformly distorted and this is consistent with past disruption of discharge from WIS (Hulbe and Fahnestock, 2007).

Minna Bluff

An extensive set of crevasses and open rifts are produced where ice outlet glaciers flowing into the RIS turns north and shears past Minna Bluff (Fig. 6). Crevasses originating at the upstream end of the bluff cut across snow-covered crevasses that originated far upstream. The new crevasses propagate eastward until they arrest near the boundary of a province containing merged suture zones from the Skelton,

https://doi.org/10.1017/aog.2017.24 Published online by Cambridge University Press

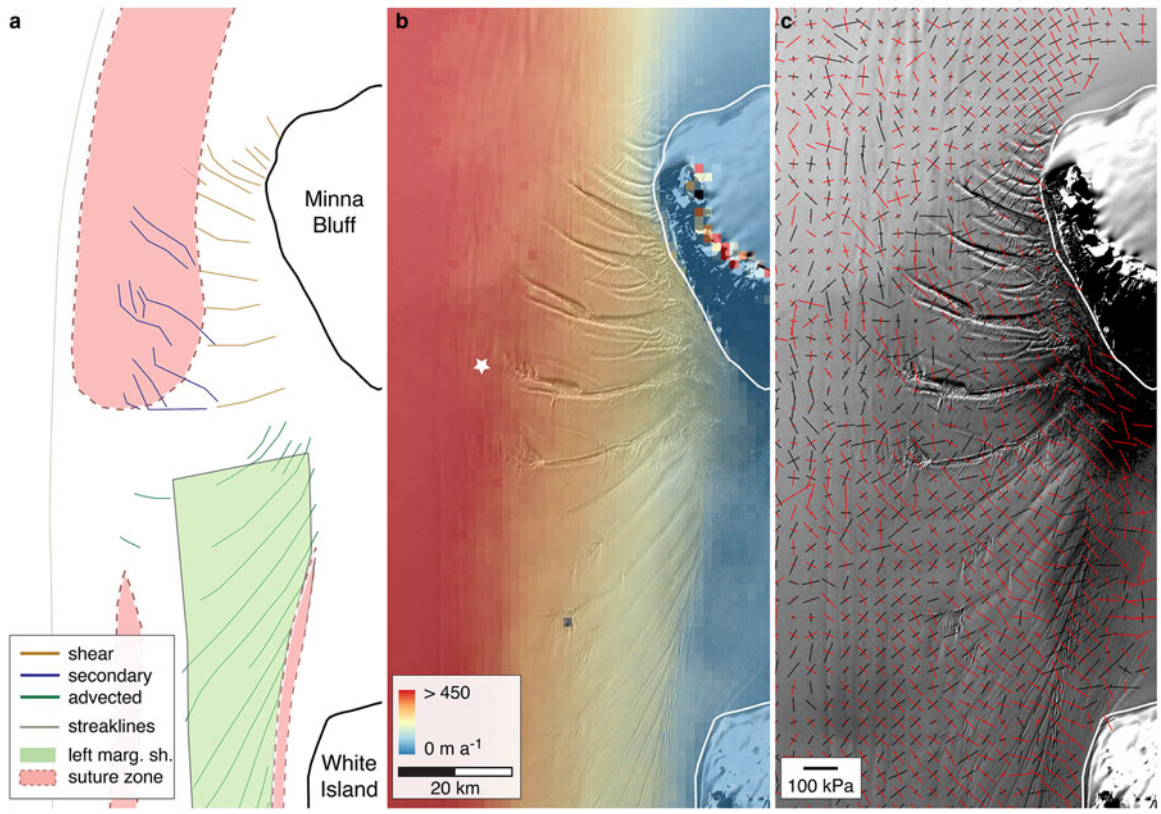

Fig. 6. The eastern side of Minna Bluff and adjacent RIS. (a) Digitized streaklines and crevasses, with interpreted structural provinces. (b) Detail of a Landsat 8 panchromatic band image, path 224 row 128, acquired 11/15/2016, courtesy of the US Geological Survey with Landsat-8-derived surface speed. The white star marks the approximate location of the British National Antarctic Expedition's 'depot A'. (c) Principal stress directions and approximate magnitudes from surface velocity plotted over the Landsat 8 image. Red indicates the compressive direction and black indicates extension.

Evtimov and Mulock Glaciers. As the initial crevasses round the corner and move past the bluff, a second episode of propagation develops. Secondary fractures with the appearance of exceptionally large horsetail fractures and wing cracks also form in this zone. The primary and secondary crevasses are all well aligned with principal stresses derived from the observed velocity. The crevasses eventually rotate into downstream-pointing orientations and become snow covered along the boundary between the McMurdo and Ross Ice Shelves (Whillans and Merry, 2001).

Active segments of the Minna Bluff crevasses align well with principal stress directions computed from the Landsat-8-derived velocities. Initial crevasse geometries at the upstream end of the region are aligned with the most compressive principal stress direction there. As the crevasses advect downstream, their orientations change such that the tips are poorly aligned with the stress field and secondary crevasses begin to propagate in the direction of compression. Farther downstream, snow-covered crevasses are rotated to downstream-pointing directions and experience compression orthogonal to their trace. The first direct measurement of ice shelf motion was made in this area, when members of Shackletons' *Nimrod Expedition* remeasured the position of 'depot A', left by the 1901–1904 *British National Antarctic Expedition* and found it to have moved about 500 yards a^{-1} (457 m a^{-1}) over the 6.5-year interval (Shackleton, 1909; Debenham, 1948). The measurement was made by triangulation using the depot's original alignment with two peaks on the bluff. A remarkably similar value (425 m a^{-1}) is obtained from Landsat 8 image correlation.

TAM coastline between beardmore and Nimrod Glaciers

Both small and large outlet glaciers discharge ice with clearly identifiable initial crevasse patterns into the RIS along the front of the TAM. The trunks and margins of larger glaciers tend to persist as individual provinces while ice from smaller glaciers is more likely to experience texture overprinting or to merge into a suture zones as it joins the ice shelf. The coastline between Beardmore and Nimrod Glaciers provides examples of both situations and demonstrates several fates for glacier shear zones once they enter the shelf (Fig. 7).

Ice discharging from Beardmore Glacier turns sharply north around Mount Hope as it enters the RIS. Ice from the glacier trunk is patterned by upstream-oriented linear features that appear to be the continuation of heavily crevassed flow stripes on the glacier surface. Ice from the left margin of the glacier advects downstream into a shear zone province, while on the right margin, an unknown basal obstruction disrupts the flow and produces a band of transverse crevasses in its wake. The headland of Lands End Nunataks produces a similar band of transverse crevasses. In both cases, the surface features rotate as they are advected downstream. Ice between the transverse crevasse provinces retains the surface texture indicative of margin-shear, but the features are rotated to a downstream-pointing direction.

The trunk of Lennox-King Glacier, northwest of Beardmore Glacier, is also characterized by a high discharge texture. In this case, the province associated with right lateral

https://doi.org/10.1017/aog.2017.24 Published online by Cambridge University Press

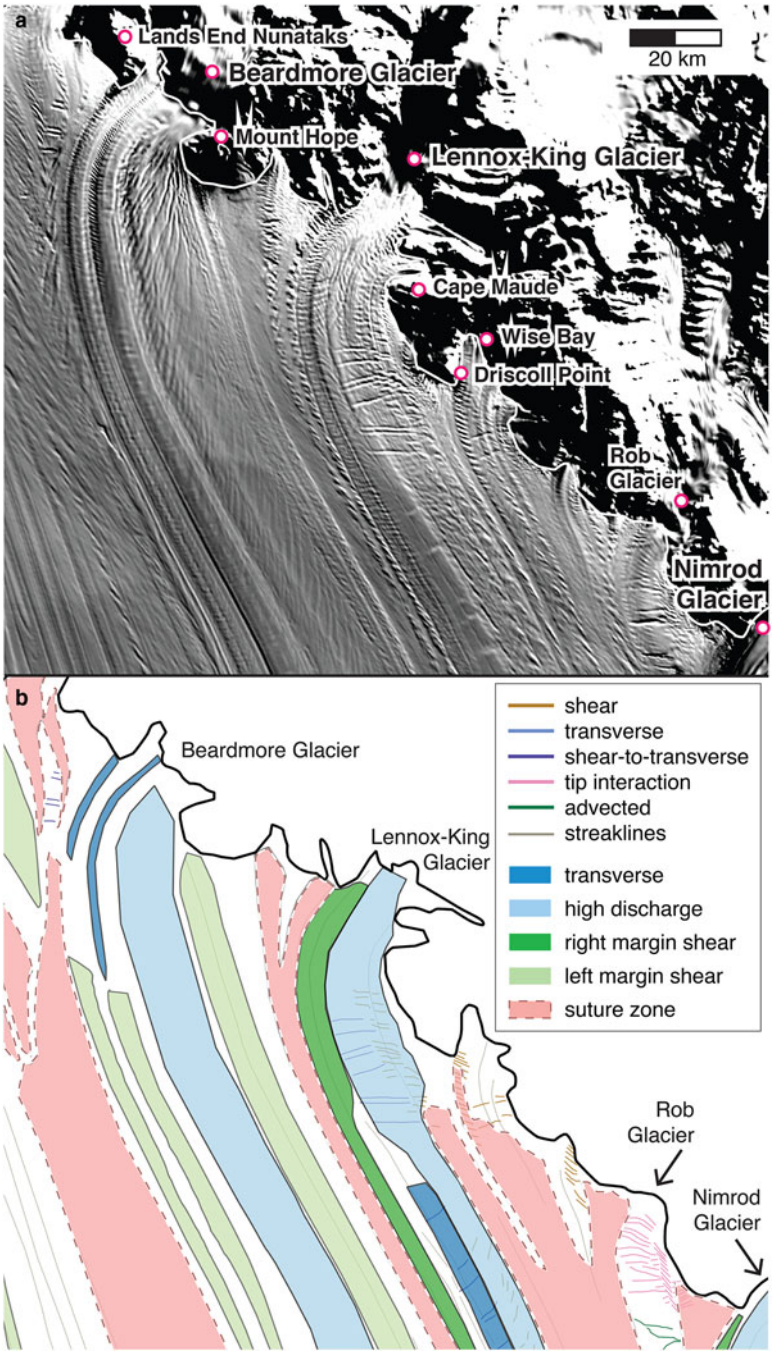

Fig. 7. Coastline of the TAM between Beardmore and Nimrod Glaciers. (a) Features as observed in the MOA. (b) Digitized streaklines and crevasses, with interpreted structural provinces.

margin-shear persists downstream, while the left lateral margin appears to merge into a suture zone with no dominant orientation. Long shear-to-transverse crevasses form where the ice turns sharply left around Cape Maude and Driscoll Point. The crevasses emerge from the left lateral margin and arrest where their tips reach ice from the right lateral margin. Another set of transverse crevasses propagate and arrest in a similar way in ice from Robb Glacier, just southeast of Nimrod Glacier.

Provinces and deformation in the ice shelf

Because they represent different upstream deformation histories, provinces imply spatial variation in ice properties, such as crystal preferred orientation (CPO), temperature and thickness. This in turn may result in spatial variation far from the ice shelf margins (Borstad and others, 2012; Hudleston, 2015). Ice thickness, and thus surface elevation, should be larger in bands emerging from glacier outlets than in the intervening suture zones. Strain rates should vary relatively smoothly across the ice shelf, except where across-flow variations in ice properties either promote or suppress deformation. We use effective strain rate and surface elevation to consider these possibilities in an exploratory way, focusing on the western part of the RIS where flow history is relatively simple (Fig. 8).

The outlets of large TAM glaciers, such as Byrd and Nimrod Glaciers, are easily identified in the effective strain rate and surface elevation maps. The lateral margins of grounded glaciers are characterized by relatively large

https://doi.org/10.1017/aog.2017.24 Published online by Cambridge University Press

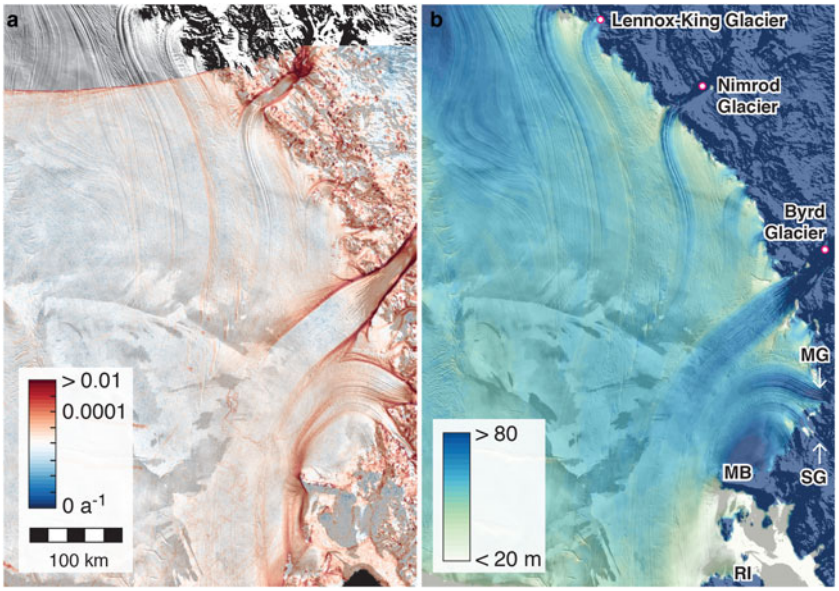

Fig. 8. The western side of the RIS. (a) Color map of effective strain rate plotted over the MOA, using a log scale. (b) Surface elevation plotted over the MOA. MG, Mulock Glacier; SG, Skelton Glacier; MB, Minna Bluff; RI, Ross Island.

effective strain rates, but once the ice is afloat, the boundary that generated large shear stresses has been left behind. Fast deformation persists in some margin-shear provinces, for example, at Byrd Glacier, while it dies away in others, for example, at Nimrod Glacier. The relatively thin (low floating) suture provinces are in some cases also characterized by relatively large effective strain rates.

Byrd Glacier appears to dominate the region of the ice shelf into which it discharges. Flow traces in the floating ice remain well aligned with the grounded glacier's orientation more than 100 km downstream and the effective strain rate remains large along the margins of the high discharge province for all of that distance. Where the province begins to turn north, the fast deformation along its margins declines abruptly. It appears that ice in strongly sheared bands at the margins of the glacier continue to deform rapidly even without supporting sidewalls as long as they maintain the same alignment relative to the principal stress directions. Additional zones of relatively large deformation rate extend both left and right of the Byrd Glaicer high discharge province. The zones have a feathery appearance, with filaments of slightly larger and slightly smaller deformation rate. The effective strain rate grows again near the front of the ice shelf, in a zone comprised of the merged left and right margins of the Byrd and Mulock Glaciers.

Ice downstream from Mulock and Skelton Glaciers is characterized by patterns similar to that observed downstream of Byrd Glacier. Margin-shear and suture zone ice deforms more rapidly than ice from the glacier trunks. Initially large effective strain rates decline as the provinces turn northward into the shelf and then grow again farther downstream. Farther south along the TAM coast, ice discharging from Beardmore and Lennox-King Glaicers turns into the shelf over shorter distances and the traces of fast-deforming margins fade more quickly in the other examples, while ice in the adjacent suture zone provinces continue to deform relatively rapidly.

All together, we conclude that these relationships are evidence that material properties associated with structural provinces affect ice deformation over large distances along flow. Where the deformation rate is large, falls and then rises again in a particular zone, as downstream of Skelton, Mulock and Byrd Glaciers, we infer that ice in the zone has a CPO that is alternately well and poorly aligned for deformation in the ambient stress field. Ice in suture zone provinces is a composite of relatively thin, and fractured ice. Because the ice is thinner (floats lower), basal meltwater rising from adjacent, deeper keeled high discharge provinces, may refreeze in these zones. Where rifts have propagated through the full thickness of the ice, sea ice and marine ice may fill the open area. Thus, these provinces may be deforming relatively rapidly because the ice is thinner, warmer or does not have a CPO that makes it relatively stiff in any location or orientation to the principal stress field.

DISCUSSION

In his 1940 review of the global state of knowledge of Antarctic glacier ice, Laurence M. Gould wrote '[p]robably no feature of Antarctic glaciology or geology has provoked as much interest among explorers and has brought forth such great variety of opinions as to their origin as the shelf ice masses' (Gould, 1940). Ice shelves continue to hold our attention, due in part to their role in mediating the progress of ice sheet response to climate change (Mercer, 1978). The origin and composition of the RIS became a subject of considerable debate from the moment sledging parties made their first journeys across its surface and here too, glaciological interest persists. Edgeworth David and Raymond Priestly, geologists on Shackleton's 1907–1909 British *Antarctic Expedition*, proposed that the RIS was a composite containing 'ribs' of relatively stiff ice emanating from TAM glaciers, draped by a surface accumulation of densifying snow. The view was later discounted, in favor of local snow accumulation (Gould, 1940). Modern satellite remote sensing of the ice shelf indicates that David and Priestly were more correct than later writers realized.

The RIS is a composite of merged flowbands containing ice with a variety of deformation histories. Some bands are characterized by distinctive surface textures and where the

https://doi.org/10.1017/aog.2017.24 Published online by Cambridge University Press

interpretation is clear, we have mapped ice-shelf structural provinces. Province configurations are relatively straightforward in the western part of the ice shelf, where flow traces conform relatively well to the present day flow field (Hulbe and Fahnestock, 2004), indicating that either TAM glaciers experience relatively small amplitude flow variation over time or that past variation is not well preserved (Hulbe and Fahnestock, 2007). It may be possible to tease information about past TAM glacier discharge variations, such as those suggested by Jones and others (2016), out of finer resolution analysis of along-flow change in structural province characteristics. In the east, even our conservative mapping indicates a more complex past behavior than is currently known, such as variations in basal traction and grounding on ice plains (Fried and others, 2014; Winberry and others, 2014).

The structural map can support a variety of additional investigations. Structural provinces imply spatial variation in ice mechanical properties and we have found some evidence of this. A more thorough investigation would require velocity data sets with smaller errors and less noise. Alternatively, these properties could be sensed remotely, using seismological approaches (Maurel and others, 2015). Downstream changes in structural province type and overprinting of crevasse patterns may be attributed to temporal changes in stress regime along a flow band. While not investigated here, we suggest that this kind of evidence may lead to new insights into past variability along the Shirase, Siple and Gould Coasts, where West Antarctic ice streams enter the RIS.

The structural province map can support new investigations into the emergence, propagation and failure of the long crevasses that produce tabular iceberg calving events. Advection through varying stress fields, interaction with adjacent fractures, and modification of the stress field by changes in the fracture itself can produce *episodic growth*, in which the fracture experiences cycles of propagation and quiescence. Episodic propagation was demonstrated quantitatively to be regulated by structural boundaries on the Ronne Ice Shelf (Hulbe and others, 2010) and we find ample evidence of the same in the present work.

CONCLUSION

We use a simple set of dominant crevasse geometries to identify provinces in the RIS that share common deformation history. Structural province formation is time dependent, so the attributes of a province must be understood in that context. Older textures may be overprinted, fractures originating in one stress regime may be modified by later episodes of propagation, and rotation in the ambient flow field can reorient surface features and underlying ice. For example, many TAM outlet glaciers turn abruptly into the ice shelf and this has different consequences in different places. In some cases, we can trace ice from lateral margins far downstream, while elsewhere the distinctive shear textures are lost over a few tens of km.

Suture zones between the margins of adjacent outlets do not have uniform characteristics. Ice from smaller outlet glaciers merges into relatively broad suture zones where original textures may be overprinted and bands of ice with many deformation histories are sandwiched together. In contrast to this, sutures between relatively large and fast flowing outlets are narrow and have no distinguishing surface texture.

Spatially variable deformation history implies spatially variable ice properties (Hudleston, 2015). Ice in a province characterized by sustained deformation of a particular type will develop a CPO compatible with that history. Ice in transverse-crevasse and high-discharge provinces experienced along-flow stretching and vertical shortening, while ice in margin-shear provinces experienced simple shear. When ice with a CPO enters the ice shelf, that fabric is retained until new conditions cause it to change, and this may make the ice either soft or stiff relative to stresses it experiences as it advects toward the calving front. We see evidence of this throughout the western part of the RIS.

ACKNOWLEDGEMENTS

LeDoux was supported by NASA Cryosphere award number NNX10AH81G. Hulbe was supported by New Zealand Antarctic Research Institute award NZARI RFP 2014-2 'Vulnerability of the Ross Ice Shelf in a Warming World'. The velocity mapping was supported by NASA Cryosphere award number NNX16AJ88G. The digitized features and province map will be archived as GIS shape files at the US National Snow and Ice Data Center and are also available by request from Hulbe and Forbes. We thank two reviewers for careful and thoughtful remarks that helped improve the manuscript.

REFERENCES

Bindschadler R and 8 others (2008) The Landsat Image Mosaic of Antarctica. *Remote Sens. Environ.*, **112**(12), 4214–4226, (doi: 10.1016/j.rse.2008.07.006)

Borstad CP and 6 others (2012) A damage mechanics assessment of the Larsen b ice shelf prior to collapse: toward a physically-based calving law. *Geophys. Res. Lett.*, **39**, L18502 (doi: 10.1029/2012GL053317)

Brunt KM, Fricker HA and Padman L (2011) Analysis of ice plains of the Filchner-Ronne ice shelf, Antarctica, using icesat laser altimetry. *J. Glaciol.*, **57**(205), 965–975

Casassa G, Jezek KC, Turner J and Whillans IM (1991) Relict flow stripes on the Ross Ice Shelf. *Ann. Glaciol.*, **15**, 132–138

Colgan W and 6 others (2016) Glacier crevasses: observations, models, and mass balance implications: glacier crevasses. *Rev. Geophys.*, **54**(1), 119–161, (doi: 10.1002/2015RG000504)

Cotterell B and Rice J (1980) Slightly curved or kinked cracks. *Int. J. Fract.*, **16**(2), 155–169, 1573–2673 (doi: 10.1007/BF00012619)

Debenham F (1948) The problem of the Great Ross Barrier. *Geogr. Jo.*, **112**(4/6), 196–212

DiMarzio (2007) GLAS/ICESat 500 m Laser Altimetry Digital Elevation Model of Antarctica (doi: 10.5067/K2IMI0L24BRJ)

Ely JC and Clark CD (2016) Flow-stripes and foliations of the Antarctic ice sheet. *J. Maps*, **12**(2), 249–259, (doi: 10.1080/17445647.2015.1010617)

Fahnestock M, Scambos T, Bindschadler R and Kvaran G (2000) A millennium of variable ice flow recorded by the ross ice shelf, Antarctica. *J. Glaciol.*, **46**(155), 652–664, (doi: 10.3189/172756500781832693)

Fahnestock M and 5 others (2016) Rapid large-area mapping of ice flow using Landsat 8. *Remote Sens. Environ.*, **185**, 84–94, (doi: 10.1016/j.rse.2015.11.023)

Fried M, Hulbe C and Fahnestock M (2014) Grounding line dynamics and margin lakes. *Ann. Glaciol.*, **55**(66), 87–96 (doi: 10.3189/2014AoG66A216)

Glasser N and 7 others (2009) Surface structure and stability of the Larsen c ice shelf, Antarctic Peninsula. *J. Glaciol.*, **55**(191), 400–410, ISSN 0022-1430 (doi: 10.3189/002214309788816597)

https://doi.org/10.1017/aog.2017.24 Published online by Cambridge University Press

Glasser NF, Jennings SJA, Hambrey MJ and Hubbard B (2015) Origin and dynamic significance of longitudinal structures ('flow stripes') in the Antarctic Ice Sheet. *Earth Surf. Dyn.*, **3**(2), 239–249, (doi: 10.5194/esurf-3-239-2015)

Gould LM (1940) Glaciers of Antarctica. *Proc. Am. Philos. Soc.*, **82** (5), 835–876

Haran T, Bohlander J, Scambos T and Fahnestock M (2005, updated 2013) MODIS Mosaic of Antarctica 2003-2004 (MOA2004) Image Map. Digital media, National Snow and Ice Data Center, Boulder, CO, USA (doi: 10.7265/N5ZK5DM5)

Herzfeld U, McDonald B and Weltman A (2013) Bering glacier and Bagley ice valley surge 2011: crevasse classification as an approach to map deformation stages and surge progression. *Ann. Glaciol.*, **54**(63), 279286

Hudleston PJ (2015) Structures and fabrics in glacial ice: a review. *J. Struct. Geol.*, **81**, 1–27, (doi: 10.1016/j.jsg.2015.09.003)

Hulbe C and Fahnestock M (2007) Century-scale discharge stagnation and reactivation of the Ross ice streams, West Antarctica. *J. Geophys. Res.*, **112**(F3), F03S27 (doi: 10.1029/2006JF000603)

Hulbe CL and Fahnestock MA (2004) West Antarctic ice-stream discharge variability: mechanism, controls and pattern of grounding-line retreat. *J. Glaciol.*, **50**(171), 471–484

Hulbe CL, LeDOUX C and Cruikshank K (2010) Propagation of long fractures in the Ronne Ice Shelf, Antarctica, investigated using a numerical model of fracture propagation. *J. Glaciol.*, **56**(197), 459–472

Jackson JA (1997) *Glossary of geology*, 4th edn. American Geological Institute, Alexandria, VA, USA

Jackson S and Kamb B (1997) The marginal shear stress of ice stream B, West Antarctica. *J. Glaciol.*, **43**, 415–426

Jezek KC (1984) Recent changes in the dynamic condition of the ross ice shelf, Antarctica. *J. Geophys. Res.: Solid Earth*, **89**(B1), 409–416, (doi: 10.1029/JB089iB01p00409)

Jones R, Golledge N, Mackintosh A and Norton K (2016) Past and present dynamics of Skelton Glacier, Transantarctic Mountains. *Antarct. Sci.*, **28**(5), 371–386, 1365–2079 (doi: 10.1017/S0954102016000195)

Khazendar A, Rignot E and Larour E (2007) Larsen b ice shelf rheology preceding its disintegration inferred by a control method. *Geophys. Res. Lett.*, **34**(19), L19503 (doi: 10.1029/2007GL030980)

Kim YS and Sanderson DJ (2006) Structural similarity and variety at the tips in a wide range of strike-slip faults: a review: similarity and variety at strike-slip fault tips. *Terra Nova*, **18**(5), 330–344, (doi: 10.1111/j.1365-3121.2006.00697.x)

Lazzara MA, Jezek KC, Scambos TA, MacAyeal DR and van der Veen CJ (1999) On the recent calving of icebergs from the Ross Ice Shelf[1]. *Polar Geogr.*, **23**(3), 201–212, 1939-0513 (doi: 10.1080/10889379909377676)

LeDoux C (2007) A boundary element model for fracture propagation in the Ronne Ice Shelf, Antarctica. Master's thesis, Portland State University, Portland, OR

MacAyeal DR and Lange MA (1988) Ice-shelf response to ice-stream discharge fluctuations: II. Ideal rectangular ice shelf. *J. Glaciol.*, **34**(116), 128–135

Martel SJ and Boger WA (1998) Geometry and mechanics of secondary fracturing around small three-dimensional faults in granitic rock. *J. Geophys. Res.: Solid Earth*, **103**(B9), 21299–21314, (doi: 10.1029/98JB01393)

Maurel A, Lund F and Motagnat M (2015) Propagation of elastic waves through textured polycrystals: application to ice. *Proc. R. Soc. A – Math. Eng. Sci.*, **471**(2177), 20140988 (doi: 10.1098/rspa.2014.0988)

McGrath D and 5 others (2012) Basal crevasses on the Larsen c ice shelf, Antarctica: implications for meltwater ponding and hydrofracture. *Geophys. Res. Lett.*, **39**(16), L16504, (doi: 10.1029/2012GL052413)

Mercer JH (1978) West Antarctic ice sheet and CO_2 greenhouse effect: a threat of disaster. *Nature*, **271**(5643), 321–325 (doi: 10.1038/271321a0)

Merry CJ and Whillans I (1993) Ice-ow features on Ice Stream B, Antarctica, revealed by SPOT HRV imagery. *J. Glaciol.*, **39** (133), 515–527

Nath PC and Vaughan DG (2003) Subsurface crevasse formation in glaciers and ice sheets: subsurface crevasse formation. *J. Geophys. Res.: Solid Earth*, **108**(B1), ECV 7-1–ECV 7-12, (doi: 10.1029/2001JB000453)

Pollard DD and Aydin A (1988) Progress in understanding jointing over the past century. *Geol. Soc. Am. Bull.*, **100**(8), 1181–1204, (doi: 10.1130/0016-7606(1988)100<1181:PIUJOT>2.3.CO;2)

Rignot E, Mouginot J and Scheuchl B (2011) Ice flow of the Antarctic Ice Sheet. *Science*, **333**, 1427–1430, (doi: 10.1126/science.120336)

Rist M, Sammonds P, Murrell S, Meredith P, Doake C, Oereter H and Matsuki K (1999) Experimental and theoretical fracture mechanics applied to Antarctic ice fracture and surface crevassing. *J. Geophys. Res.*, **104**(B2), 2973–2987

Shackleton EH (1909) Some results of the British Antarctic Expedition, 1907-9. *Geogr. J.*, **34**(5), 481, ISSN 00167398 (doi: 10.2307/1777278)

Van der Veen CJ (1999) *Fundamentals of glacier dynamics*. A. A. Balkema, Rotterdam

Whillans IM and Merry CJ (2001) Analysis of a shear zone where a tractor fell into a crevasse, western side of the Ross Ice Shelf, Antarctica. *Cold Reg. Sci. Technol.*, **33**(1), 1–17, (doi: 10.1016/S0165-232X(01)00024-6)

Winberry JP, Anandakrishnan S, Alley RB, Wiens DA and Pratt MJ (2014) Tidal pacing, skipped slips and the slowdown of Whillans ice stream, Antarctica. *J. Glaciol.*, **60**(222), 795–807, ISSN 0022-1430 (doi: 10.3189/2014JoG14J038)

https://doi.org/10.1017/aog.2017.24 Published online by Cambridge University Press